Functional Materials 17, No.1 (2010)

Magnetic oscillations of longitudinal sound in iron borate

V.I.Khizhnyi, V.V.Tarakanov, T.M.Khizhnaya

O.Usikov Institute for Radiophysics and Electronics, National Academy of Sciences of Ukraine, 12 Akad. Proskura St., 61085 Kharkiv, Ukraine

Received October 12, 2009

The amplitude and phase of longitudinal acoustic wave transmission coefficient in a single-crystal $FeBO_3$ plate under its magnetization in an external magnetic field have been experimentally investigated at frequencies about 200 MHz. The oscillations in magnetic field dependences of attenuation and phase velocity have been discovered in $\mathbf{H}\perp\mathbf{q}\|C_3$ geometry (**H** is the external magnetic field; **q**, the sound wave vector; C_3, the crystal trigonal axis). Their behavior as a function of frequency and temperature has been studied. A possible interaction mechanism between longitudinal sound and magnetic system in strained $FeBO_3$ crystal has been proposed. It is connected with the occurrence of magnetic modulation structure having a period comparable with the sound wavelength. The result of numerical simulation carried out agrees qualitatively with the experimental data.

На частотах ~200 МГц экспериментально исследованы амплитуда и фаза коэффициента прохождения продольных акустических волн в монокристаллической пластинке $FeBO_3$ при ее намагничивании во внешнем магнитном поле. В геометрии $\mathbf{H}\perp\mathbf{q}\|C_3$ (**H** — внешнее магнитное поле, **q** — волновой вектор звука, C_3 — тригональная ось кристалла) обнаружены осцилляции магнитополевых зависимостей затухания и фазовой скорости. Исследовано их поведение в функции частоты и температуры. Предложен возможный механизм резонансного взаимодействия продольного звука с магнитной системой в напряженном кристалле $FeBO_3$. Он связан с возникновением магнитной модуляционной структуры с периодом, соизмеримым с длиной волны звука. Результат проведенного численного моделирования качественно согласуется с экспериментальными данными.

1. Introduction

The peculiarities of dynamic magnetoelastic (ME) coupling in antiferromagnets ("weak" ferromagnets) with the easy-plane type of magnetic anisotropy (AFEP) are of substantial physical interest, because the AFEP have a strong ME coupling due to an "exchange amplification" effect [1]. As a result of strong ME coupling, the dynamic and static elastic deformations may change the crystal magnetic properties, which is very attractive from the viewpoint of its applications in acousto-optics and acoustoelectronics. Up to date, similar types of effects at high ultrasound frequences were insufficiently studied in experiment for $FeBO_3$ AFEP.

In iron borate ($FeBO_3$), the propagation of transversely polarized sound in external magnetic field at $\mathbf{H}\perp\mathbf{q}\|C_3$ (C_3 is the trigonal axis normal to the {111} basal plane of the crystal) has been studied by authors in [2, 3]. In those works, the high-frequency acoustic magneto-polarization effects were revealed and their peculiarities connected with mechanical boundary conditions were studied. In [4], the linear generation of the longitudinal sound by an alternative magnetic field

was discovered, indicating a connection between magnetic system and the longitudinal acoustic wave at $\mathbf{q} \| C_3$. The latter fact is of a special interest, as a relativistic magnetostriction coupling between the longitudinal elastic oscillations along C_3 and magnetic subsystem is negligibly small due to a large energy gap for the high-frequency branch of spin-wave spectrum [5]. In addition to the magnetostriction part to energy $F_{me} \sim B_{ijkl} l_i l_j e_{kl}$, it is necessary to take into account a piezomagnetic (PM) one $F_{pm} \sim P_{ijkl} m_i l_j e_{kl}$, where B and P are the striction and PM constants, respectively; e_{kl}, the elastic strain tensor; m_i, the component of magnetization vector $(\mathbf{m} = (\mathbf{M_1} + \mathbf{M_2})/2M_0)$; l_i, the component of antiferromagnet vector $(\mathbf{l} - (\mathbf{M_1} - \mathbf{M_2})/2M_0)$; $\mathbf{M_1}$ and $\mathbf{M_2}$, the magnetization vectors of the first and the second magnetic sublattices; M_0, the equilibrium magnetization of them. Note that the piezomagnetism describes the linear in H coupling of magnetization $\mathbf{m}$ and the longitudinal deformation e_{zz} (along C_3 axis). In addition, if there are external mechanical strains at the sample surface in the basal plane (XY), then equilibrium deformations e_{zz} due to the PM-coupling are functions of both σ_{zz} and σ_{xx}, σ_{yy} [1].

The purpose of this work is to study the influence of PM coupling on the conditions of longitudinal acoustic wave propagation in a $FeBO_3$ crystal in external magnet field.

2. Experimental

The iron borate samples with half-width line of AFMR less than 100 Oe at $T = 77$ K and frequency 60 GHz, were used. The samples were grown by spontaneous crystallization from solution in melt. Those were shaped as platelets. Their developed surfaces were parallel to the crystal basal {111} plane. The surface area of platelets was about 10 mm^2 and platelet thickness d, about 70 to 140 μm. Some samples having grown rolls at the surfaces were prepolished using abrasive powders.

The measuring cell is the composite acoustic resonator (CAR) [6]. The CAR consists of the sample, a pair of single-mode $LiNbO_3$ piezotransducers (PZT) for longitudinal sound and the screening silvered copper spacers. The measuring cell sandwich structure is optimized to prevent a HF-leakage on PZT. The PZT are fixed between the screening spacers using spring-loaded clamping contacts. The spring is made of beryllium bronze. According to our estimates, the pressure force on PZT of 2 mm diameter does not exceed 30 to 40 g. The possible pressure changes during the measurements have not been checked. As an acoustic contact, fluid SGF or Nonaq Stopcock Grease paste are used. The measurements have been made using the resonance interferometric technique in the continuous-wave mode. In detail, the measuring method has been described in [6]. Here, the following is to be noted. The CAR and low-noise pre-amplifier are situated in the measuring channel of vector-meter (a FK2-12 phase-meter). It records the signal amplitude in the measuring channel in "on pass" mode and the phase difference between signals of measuring and reference channels. The mechanical frequency tuning of the generator provides the measuring of the amplitude-frequency (AFC) and phase-frequency (FFC) characteristics for the measuring cell in the frequency range of the PZT HF-electrical matching. There was a possibility to use phase-meter as "zero" phase indicator. All data are set into PC for a subsequent digital processing.

The measuring process consisted of several stages. Initially, the AFC and FFC have been measured for a specified sample, the PZT sets and series of measurements at the frequency range of mechanical Fabry-Perrot (FP) resonance using a sample at $H = 0$. Then, according to [6], the discrete operation frequences of FP-resonances f_n (at $H = 0$) have been selected. These frequences are used for the subsequent measurement of amplitude U and phase Ψ of transmission coefficient as a function of H. Thereafter, takind the calibrations into account and using a software, the relative values $U(H)/U(0) \approx -\Gamma(H)/\Gamma(0)$ and $\Delta f(H)/f_n = -\Delta\upsilon/\upsilon$ (Γ is the of sound attenuation coefficient; $\upsilon \approx 8.4 \cdot 10^5$ cm/s is the longitudinal sound phase speed) have been obtained. These data are tested by a direct measurement of quality factor variation ΔQ (or $\Delta U(H)$ and $\Delta f(H)/f_n$) with the phase-meter being in the "zero-indicator" mode at some selected H values. For example, at room temperature and a given set of PZT, the CAR was matched at the level of voltage standing-wave ratio (VSWR) ~ 1.5 in frequency range of 180–240 MHz. This level of VSWR provides the observation of three successive FP-resonances numbered as $n = 2f_n d/\upsilon = 6$ to 8 ($Q \sim 100$), where d is the sample thickness ≈140 μm. In this case, the FP-resonances with $n = 6$, 8, having a linear FFC in the frequency deviation range $\Delta f = f(H) - f_n$,

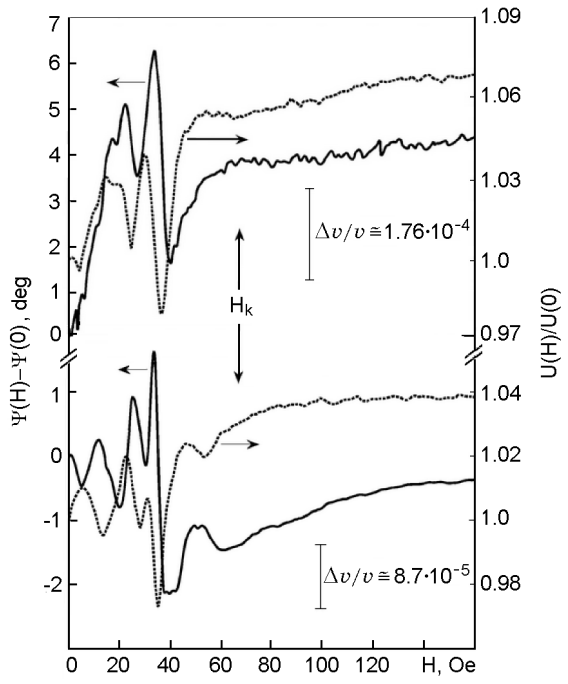

Fig. 1. Magnetic field dependences of transmission coefficient phase and amplitude for longitudinal acoustic wave at $T = 300$ K, $f \approx 181$ MHz. $C_2 \perp H$ (the upper curves) and $C_2 \| H$ (the bottom curves).

are selected for measurement. The measurement error does not exceed 0.2 % for $\Delta U/U$ and 10^{-5} for $\Delta f/f$. For temperature measurements at $T > 300$ K, the measuring cell is placed in a thermostat and for 77 K $< T <$ 300 K, in a cryostat with pumping of nitrogen vapor. The magnetic field is created by Helmholtz coils allowing to orientate the **H** vector in the sample basal plane over the range of 0°–180°. The positioning error of **H** relative to the sample symmetry axes was not exceeded 2 to 3°.

3. Experimental results

For systematic measurements, the $d \approx 140$ μm thick samples have been chosen. In Fig. 1, amplitude and phase of the acoustic wave transmission coefficient upon a magnetization cycle in field up to 160 Oe are presented. The upper curves correspond to the $C_2 \perp H$ geometry, the bottom ones, to $C_2 \| H$ (C_2 being the two-fold axis lying in the basal plane). The signal amplitude and phase (i.e. the sound attenuation and speed) are seen to vary in oscillatory manner as H increases. That oscillating structure exists in the limited field range $0 < H < H_K$ (where H_K is the field where the oscillations disappear). The maximal oscillation amplitude excursion has been obtained at H ~ 40 Oe. Against the background of oscillations in Fig. 1, there is a monotonous line corresponding to the sound attenuation decreasing with increasing H. The relative amplitude change in maxima attains 7 %, and corresponds to the relative change in the sound phase velocity of $\Delta\upsilon/\upsilon \approx 4 \cdot 10^{-4}$ for both magnetic field directions.

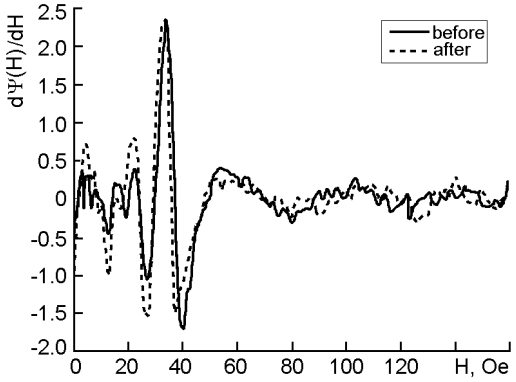

Fig. 2. Magnetic field derivative of phase with respect to magnetic field for $C_2 \perp H$. The curves "before" and "after" are recorded prior to and after the sample magnetization in field up to 350 Oe, respectively.

In field dependences, the peculiarities appear just starting from $H = 0$ where a domain structure exists. So, to study the influence of domain walls (DW) shift on the acoustic signal passage, the evolution of line shape after the sample magnetization in the field $H_m >> H_s$, where H_s is the field of single-domain sample (for the samples under study, H_s ~ 10–20 Oe at $T = 300$ K, and $H_s \leq 40$ Oe at $T = 77$ K [4]) was investigated. The same protocol was used in [7] when electromagnetically studying the natural resonances of DW. As an example, Fig. 2 shows the phase derivative with respect to magnetic field (the case $C_2 \perp H$) prior to and after the sample magnetization in the field $H_m = 350$ Oe. The influence of domain structure changes on the longitudinal sound propagation conditions is seen to be appreciable in the H range of 0 to ~20 Oe. In this field region, the shape and number of oscillations are changed, while no changes are observed at $H > 20$ Oe. It should be noted that the sample magnetization reversal (i.e. $+H$ to $-H$) in field up to 160 Oe gave the same result, i.e. the hysteresis took place at $H \leq 20$ Oe. The fact of the hysteresis existence denotes a coupling between longitudi-

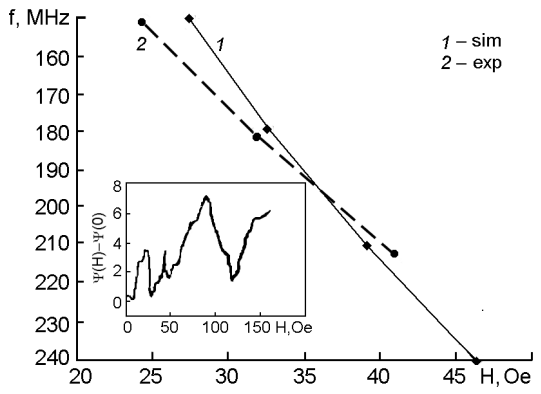

Fig. 3. Position of $\Psi(H)$ maxima vs frequency for the case $C_2 \| H$ (the curve "exp" is experimental, the curve "sim" is numerically simulated). The inset presents the magnetic field dependence of transmission coefficient phase at $f \approx 244$ MHz.

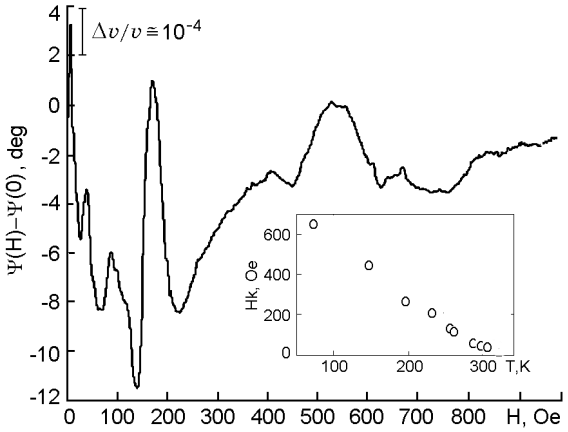

Fig. 4. The transmission coefficient phase vs magnetic field at $T = 77$ K, $C_2 \| H$, $f =$ 184.3 MHz. The inset presents dependence of H_K on T.

nal sound wave and magnetic non-uniformities (domains).

To reveal the spectrum of observed peculiarities in magnetic field, the field dependences have been measured at the four FP-resonances frequences $n = 5$, 6, 7, 8 (~150, ~180, ~210, and ~240 MHz). A typical spectrum in field H is shown in Fig. 3 (the curve "exp") for $C_2 \perp H$ geometry (taken in the point of $\Psi(H)$ maximum, Fig. 1). It is seen that the increasing frequency shifts the maximum towards stronger fields and vice versa. Unfortunately, this method is used at the sample mechanical resonance frequences only, and does not allow to take the spectrum at the small frequency variation steps. For example, at frequency ~ 240 MHz ($n = 8$), there is some selection ambiguity in the spectrum experimental points due to a rather complicated picture of oscillations, which are presented for phase at the inset in Fig. 3. Therefore, the spectrum point for ~240 MHz and H ~ 90 Oe, was discarded. According to the inset, this resonance peculiarity is similar in shape to that at H ~ 40 Oe, but has a larger line width. Let to note that the spectral dependences had the same character at the $C_2 \| H$ geometry.

In contrast to the frequency change, the influence of temperature variation on a magnetic field position of amplitude and phase oscillations appears to be a more substantial. Upon temperature decreasing, the increasing oscillation period in field H is observed. In Fig. 4, the field dependence of the signal phase at $T = 77$ K, $f =$ 184.3 MHz ($n = 6$) and $C_2 \| H$ is shown. The inset in Fig. 4 presents the temperature dependence of field H_K. The comparison of Fig. 1 and Fig. 4 indicates that the decreasing temperature substantially expands the magnetic field region where oscillations are observed, but does not change their number. The temperature increasing above 300 K results in decreasing both H_K and the magnitude of phase and amplitude variation in magnetic field. For $T \geq 320$ K, the magnitude of all peculiarities falls down to noise level, so those are not observed at $H >$ 20 Oe against the background of monotonous behavior. The Neel point for iron borate is $T_N = 348$ K.

The next factor affecting the magnetic field peculiarities is the azimuth angle φ_H between the external magnetic field H vector and the two-fold axis direction in the basal plane. The above-shown dependences are taken at $\varphi_H = 0°$ and 90°. As noted above, in a single-domain sample (at $H >$ 20 Oe) the field inversion does not change the observed dependences. Therefore, the evolution of azimuth dependences over the range $\varphi_H = 0°$ to 180° at the step $\Delta\varphi_H = 5°$ has been studied. The shape and position of oscillations in magnetic field as well as their monotonous component depend substantially upon φ_H. Non-monotonies in amplitude-phase dependences exist for all H orientations in the basal plane. In this connection, a variation of basal anisotropy for the signal amplitude and phase due to a pressure and inhomogeneous strains of the sample are observed. The influence of mechanical boundary conditions, in particular upon of the sample reinstallation ("allocation") into the measuring cell is revealed.

As noted above, it is impossible to change considerably the pressure on the sample. However, it has been revealed that monotonous trend of curves (see Fig. 1) (especially for amplitude) is sensitive to the sample "allocation". The same concerns to a lesser degree the shape and position of peculiarities in magnetic field. For example, the higher is the pressure, the higher the slope of monotonous trend is for all curves in Fig. 1. Such being the case, the relative change of signal amplitude in resonance field exceeds ~20 % and dispersion of sound velocity is $\Delta\upsilon/\upsilon \approx 5\cdot10^{-4}$. This evidences also a significant influence of mechanical loading on characteristics of discovered effects. At a given experimental arrangement, any control of sample pressure was absent due to hard conditions of PZT screening. For the same reason, several repetitive sample "allocations" are necessary to reproduce the field dependences. The detailed study of these effects will be published in a separate article.

4. Discussion

As is evidenced by the observed magnetic field dependences of amplitude and phase of the longitudinal sound transmission coefficient, there is a coupling between elastic and magnetic subsystems. The ME coupling depends upon state of magnetic system through the parameters such as frequency, temperature, angle φ_H, as well as static and dynamic strains (i.e., on tensor e_{kl}). The changes in magnetic system result in an appropriatee acoustic response.

Let the possible reasons for these effects on the longitudinal sound be considered.

(i) Mutual conversion of longitudinal and transverse sound modes. Without considering the mode transformation sources, it is to note that in this case, the oscillation structure should exist within the whole range of studied field H due to a strong magneto-polarization effect accompanying the transverse sound propagation in iron borate [2].

(ii) Pinning effects of Bloch-type DW at the sample structure defects in magnetic field. A DW vibrates about the steady position at the frequency $\omega = (\alpha/m)^{1/2}$ [8], where α is the coefficient depending on local conditions of a specific crystal [9]; m is the DW mass. It is obvious that the resonance effects are possible under coincidence of ω and the sound frequency. The natural frequency of DW vibrations is rather low. According to [9], even for Neel DW with the energy $3\cdot10^{-2}$ erg·cm^{-2}, which is one order higher than the Bloch DW energy, it is ~100 MHz. In principle, this frequency may be increased upon the pinning due to increasing α [10]. But for iron borate samples the Bloch DW pinning did not observed. The experimental data on sample magnetization described above (Figs. 1, 2, 4) indicate that the acoustic oscillation (resonance) effects arise in the sample state close to the single-domain one at $H \le H_s$, and they exist up to field H_K. From one experiment to another, the impact of domain structure changes in a very low field seem to result in irregular (random) field dependences in the propagation behavior of longitudinal sound wave. The DW shift in field H increases the dissipation in an acoustic wave and DW disappearance results in decreasing of dissipation.

(iii) Magnetoacoustic dimensional resonance on a magnetic modulation structure (MMS). The essence of this mechanism is as follows. The field dependence of resonance peculiarity positions in the field (Fig. 3) indicates their possible dimensional nature. Let a space modulation of magnetic properties be assumed in the medium along **q**, i.e. the vector **m** shows periodic (or quasi-periodic) variations (alternations) along **q** with some period $2D$. Then, if there is a substantial ME-coupling, the elastic properties (acoustic impedance) of the medium will be modulated with the same period. Whenever the following condition is met:

$$2D \sim 2\pi/q, \qquad (1)$$

a sound resonance with MMS should be expected. This mechanism was suggested for the first time in theoretical work [11]. Let this effect be considered in more detail. Today, the MMS (incommensurate structures, magnetic ripples, etc.) in magnetic materials are studied both in experiment and theoretically. There are several reasons for MMS formation in nonmetallic crystals. Those may be associated with inhomogeneous relativistic and exchange interactions, as well as to a combination thereof. The MMS in iron borate is also revealed and is at present under intense investigation. In connection with interpretation of data obtained here, it is to note the following results of magnetooptic experiments in iron borate. In [13], the MMS appeared under light action in the crystal doped with diamagnetic nickel ions. Along with other effects, the impurity introduction produced a

lattice deformation in volume of crystal. The magneto-elastic (spin-phonon) mechanism of phase transition into a modulated state had been suggested. According to [12], for $FeBO_3$:Ni, $2D(H) \sim 100$ μm in field $H \sim 40$ Oe. In [14], the random deformation in an iron borate crystal were introduced by an external source (a copper washer glued to the crystal basal surface). Similar to [13], a superstructure was observed in [14] in the basal plane at magnetic field $H > 10$ Oe, with $2D(H) \sim 40–80$ μm. According to [14], the modulation of the crystal magnetic order was due to a space-inhomogeneous magnetic anisotropy induced in the crystal easy plane. In magnetooptic experiments [15], the dependence $2D$ on the sample thickness along anisotropy axis C_3 was observed. It is to emphasize especially that $2D$ period in iron borate decreased with increasing H so that $(\pi/D)^2 \sim H$ [13, 14]. If we suppose that in our experiments the condition (1) is satisfied at a certain field H, then, according to Fig. 3, the decreasing sound wavelength shifts the resonance towards a stronger field. Thus, the MMS period is decreased with increasing magnetic field. Taking these circumstances into account and following to [11], at qualitative level let the sound wave propagation be considered in a medium with MMS, where a ME coupling causes a periodical acoustic impedance modulation. The AFM of AFEP types ($FeBO_3$) with an inversion center were not considered in [11]. A theory of sound wave propagation in spiral and umbrella-like magnetic structures existing along an anisotropy axis for uniaxial AFM and FM had been given. In our opinion, the main physical result, namely the appearance of band spectrum for spin and acoustic waves, as well as an intense magnon-phonon resonance, have an universal character for others MMS with a strong ME bonding.

5. Numerical simulation

For numerical simulation, a very simple model has been chosen. Let a superstructure to exist along $q \| C_3$ vector, and the plane-parallel sample platelet of thickness d is the medium showing a periodically modulated acoustic impedance under the meander law. The sample with layers of thickness $D < d$ has the alternate impedance $Z \pm \Delta Z (\Delta Z/Z = \Delta\upsilon/\upsilon)$, where Z is the acoustic impedance of

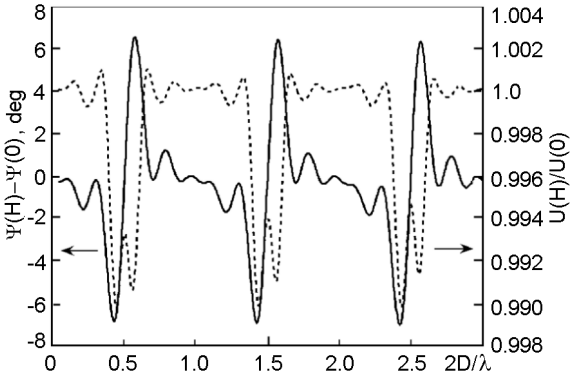

Fig. 5. Calculated dependences of transmission coefficient phase and amplitude vs $2D/\lambda$ in a platelet with number of layers $N = 5$.

iron borate ~$36 \cdot 10^6$ kg/m^{2}s. Let the mechanical loads at the sample faces to be the semi-infinite low-impedance media providing a loaded Q factor, which corresponds to an experimental one. In magneto-optic experiments, a localized (small) area of the sample surface is investigated. In current experiments, the acoustic response of the sample volume is registered. Therefore, there is some ambiguity in the choice of $2D(H)$ variation law, the harmonics and sub-harmonics of main resonance (1) are possible as well as there is a priori uncertain scenario for layers behavior in field H. This experiment suggests that the layers are compressed as the field increases. We have simulated several scenarios: the fixed and variable number of layers N ($N = 3$ to 9), the contraction tooking place both to the sample center (a symmetric case) and to its end faces (an asymmetric case). The calculation procedure and main calculation formulas are similar to those in [6, 16]. Let the results be presented being in the best agreement with experimental data. In Fig. 5, the calculated dependences of the transmission coefficient amplitude and phase at constant number of layers ($N = 5$; 2.5 periods; asymmetric case and $\Delta Z/Z = 5 \cdot 10^{-3}$) on $2D/\lambda$ ratio (where λ is the sound wavelength) are presented. In agreement with (1), the amplitude maxima take place at $2D = L\lambda$ ($L = 1$, 2:), and the minima at $2D = (L - 1/2)\lambda$. In Fig. 6, the field dependence of the signal amplitude and phase at frequency $f = 180$ MHz ($n = 6$) are shown (the rest of calculated parameters are the same as in Fig. 5). The calculated results (see Fig. 6) are obtained under assumption that layers are compressed according to the law presented in the inset in Fig. 6.

It corresponds to the following field dependence of squared MMS wave vector

$$\left(\frac{\pi}{D}\right)^2 \sim \eta H, \qquad (2)$$

where $\eta = 2.3 \cdot 10^5$, if $[H]$ is in Oersteds; $[D]$, in cm. The same law (2) was observed in [13, 14].

There is a good qualitative agreement between calculation (Fig. 6) and experiments (Figs. 1, 2), that is rather unexpected for our rough model. As in the experiment, there is a fine structure of resonance lines. The calculated spectrum in field H for resonance (Fig. 6) is presented in Fig. 3 (the curve "sim"). It is in a good enough agreement with experimental one for the 150–210 MHz frequency range. The discrepancy at the edges of this range does not exceed ~3 Oe. The appearance of an additional resonance structure in low fields (see inset in Fig. 3) can be explained by resonances with $L > 1$ appearing at decreasing sound wavelength. A more significant discrepancy between experiment and calculation takes place for spectrum in field H at $f >$ 210 MHz. In this connection, it is to note that according to [11], a spin wave may be excited in MMS under certain conditions with the linear dispersion law $\omega(k)$. Its phase velocity ω/k depends upon H. If H verge towards H_R, where H_R is the resonance condition $\upsilon = \omega/k$, the hybridization of spin and acoustic modes takes place. Therefore, in addition to the sound interference on superstructure, the effects of the two spin-phonon modes interference can be observed in these fields. At $H = H_R$, the magnon-phonon resonance may exist. Generally speaking, these phenomena depend upon sample temperature and sound frequency. Unfortunately, the theory of this effect is given in [11] only schematically, therefore, it is impossible to make estimates and qualitative comparison with experimental data.

In conclusion, it will be noted that at the simulation, we have observed effects typical for a phonon crystal. For example, the signal amplitude attenuation in a suppression band ≥12 dB for $\Delta Z/Z \geq 0.1$.

Thus, the presented results of numerical simulation argue for the consistency of our model of sound wave and MMS interaction in iron borate.

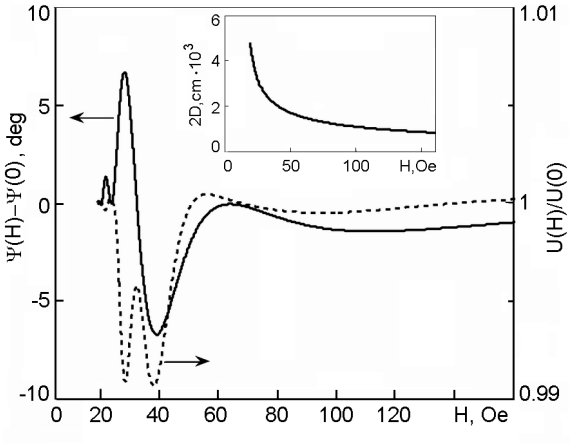

Fig. 6. Calculated dependences of transmission coefficient phase and amplitude vs magnetic field for $f = 180$ MHz. In the inset, the calculated law of $2D$ variation vs H is shown.

For the physical interpretation of data obtained, we have assumed the MMS existence within the temperature range 77 K $< T <$ 310 K. While not discussing the symmetry aspect of the problem [17], we suppose that the main cause of MMS initiation is the mechanical load of the sample giving rise to an inhomogeneous nonuniform its static deformation along C_3-axis. In addition, the inhomogeneous dynamic deformaton of the lattice, i.e. nodes and antinodes of standing acoustic wave along C_3-axis are of great importance.

6. Conclusions

In this work, the amplitude and phase of transmission coefficient for longitudinal acoustic wave in a $FeBO_3$ crystal in weak magnetic fields are measured. The interaction of longitudinal sound with magnetic subsystem is revealed. In single-domain sample state, the resonance peculiarities of attenuation and sound velocity dispersion are discovered. The temperature (77 K–320 K) and frequency (150–240 MHz) dependences thereof are investigated. Basing on experimental data and numerical simulation, it has been concluded that a MMS may exist along the C_3-axis of the crystal anisotropy. A resonance interaction mechanism between the longitudinal sound and MMS has been proposed which was considered theoretically before in [11]. Since at present, there are no experimental data on observation of a such MMS type, this work can stimulate both experimental and theoretical further studies of the problem.

Acknowledgements. The authors are grateful to Prof. A.P.Korolyuk for valuable discussions and to Dr. M.B.Strugatsky for supplying high-quality iron borate samples.

References

1. E.A.Turov, V.G.Shavrov, *Fiz.Tverd.Tela*, **7**, 217 (1965).
2. A.P.Korolyuk, V.V.Tarakanov, V.I.Khizhnyi et al., *Fiz.Nizk.Temp.*, **22**, 708 (1996).
3. Yu.N.Mitsay, K.M.Skibinsky, M.B.Strugatsky et al., *J.Magn.Magn.Mater.*, **219**, 340 (2000).
4. V.I.Khizhnyi, V.V.Tarakanov, A.P.Korolyuk et al., *Fiz.Nizk.Temp.*, **32**, 638 (2006).
5. V.G.Baryakhtar, M.A.Savchenko, V.V.Gann et al., *Zh.Eksp.Teor.Fiz.*, **47**, 1987 (1964); V.I.Ozhogin, *Izv.AN SSSR, Ser.Fiz.*, **42**, 1625 (1978).
6. V.I.Khizhnyi, V.V.Tarakanov, T.M.Khizhnaya, *Telecommunications and Radio Engineering*, **68**, 451 (2009).
7. E.I.Boyd, J.I.Budnick, L.J.Bruner et al., *J. Appl.Phys.*, **32**, 2484 (1962).
8. S.Chikazumi, Physics of Ferromagnetism, Wiley, New York, 1964 (Mir, Moscow,1967 - in Russian).
9. G.B.Scott, *J.Phys.D:Appl.Phys.*, **7**, 1574 (1974).
10. A.Hirai, J.A.Eaton, C.W.Searle, *Phys.Rev.B*, **3**, 68 (1971).
11. K.B.Vlasov, V.G.Baryakhtar, E.P. Stefanovsky, *Fiz.Tverd.Tela*, **15**, 3656 (1973).
12. Yu.A.Izyumov, *Usp.Fiz.Nauk*, **144**, 439 (1984).
13. Yu.M.Fedorov, A.F.Sadreyev, A.A.Leksikov, *Zh.Eksp.Teor.Fiz.*, **93**, 2247 (1987).
14. B.Yu.Sokolov, *Pis'ma J.Eksp.Teor.Fiz.*, **83**, 439 (2006); S.P.Boidedaev, B.Yu.Sokolov, *Zh. Tekhn.Fiz.*, **78**, 139 (2008).
15. A.V.Chzhan, T.N.Isaeva, *Fiz.Tverd.Tela*, **38**, 2461 (1996)
16. L.M.Brehovskih, O.A.Godin, Acoustics of Stratified Media, Nauka, Moscow (1989) [in Russian].
17. Yu.D.Zavorotnev, L.I.Medvedyeva, *J.Magn. Magn.Mater*, **321**, 231 (2009).

Магнітні осциляції поздовжнього звуку у бораті заліза

В.І.Хижний, В.В.Тараканов, Т.М.Хижна

На частотах ~ 200 МГц експериментально досліджено амплітуду та фазу коефіцієнту проходження поздовжніх акустичних хвиль у монокристалічній пластинці $FeBO_3$ при її намагнічуванні у зовнішньому магнітному полі. У геометрії $\mathbf{H}\perp\mathbf{q}\|C_3$ ($\mathbf{H}$ — зовнішнє магнітне поле, $\mathbf{q}$ — хвильовий вектор звуку, C_3 — тригональна вісь кристала) виявлено осциляції магнитопольових залежностей затухання та фазової швидкості. Досліджено їх поведінку у функції частоти й температури. Запропоновано можливий механізм резонансної взаємодії поздовжнього звуку з магнітною системою у напруженому кристалі $FeBO_3$. Він пов'язаний з виникненням магнітної модуляційної структури з періодом, сумірним з довжиною хвилі звуку. Результат виконаного числового моделювання якісно узгоджується з експериментальними даними.